Transcytosis of NgCAM in epithelial cells reflects differential signal recognition on the endocytic and secretory pathways

Eric Anderson, Sandra Maday, Jeff Sfakianos, Michael Hull, Bettina Winckler, David Sheff, Heike Fölsch, and Ira Mellman

Department of Cell Biology, Ludwig Institute for Cancer Research, Yale University School of Medicine, New Haven, CT 06520

NgCAM is a cell adhesion molecule that is largely axonal in neurons and apical in epithelia. In Madin-Darby canine kidney cells, NgCAM is targeted to the apical surface by transcytosis, being first inserted into the basolateral domain from which it is internalized and transported to the apical domain. Initial basolateral transport is mediated by a sequence motif (Y_{33}RSL) decoded by the AP-1B clathrin adaptor complex. This motif is a substrate in vitro for tyrosine phosphorylation by p60src, a modification that disrupts NgCAM's ability to interact with clathrin adaptors. Based on the behavior of various NgCAM mutants, it appears that after arrival at the basolateral surface, the AP-1B interaction site is silenced by phosphorylation of Tyr_{33}. This slows endocytosis and inhibits basolateral recycling from endosomes, resulting in NgCAM transcytosis due to a cryptic apical targeting signal in its extracellular domain. Thus, transcytosis of NgCAM and perhaps other membrane proteins may reflect the spatial regulation of recognition by adaptors such as AP-1B.

Introduction

The generation and maintenance of cellular polarity is an essential aspect of multicellular life. In complex tissues, individual cells organize their surface components into distinct plasma membrane domains that conduct tissue-specific functions. The best-studied polarized cell types are epithelial cells, which polarize into apical and basolateral domains, and neurons, which polarize into axonal and somatodendritic domains.

In most epithelial cells, the majority of apical and basolateral membrane components are sorted in the biosynthetic pathway, being selectively accumulated in transport carriers that are delivered to the appropriate plasma membrane domain (Drubin and Nelson, 1996; Nelson and Yeaman, 2001; Stein et al., 2002). As many membrane proteins are subsequently internalized by endocytosis, they must be continuously resorted in endosomes to maintain their polarized distributions (Mellman, 1996).

Basolateral targeting signals are most often present in the cytoplasmic tails of transmembrane proteins (Casanova et al., 1991; Hunziker et al., 1991; Matter and Mellman, 1994; Matter, 2000; Mostov et al., 2000; Koivisto et al., 2001). Sometimes colinear with clathrin-coated pit localization signals, basolateral signals often involve tyrosine- or dileucine-based motifs (Matter and Mellman, 1994; Bonifacino and Traub, 2003). Many basolateral signals are decoded by the epithelial cell-specific clathrin adaptor complex AP-1B (for reviews see Fölsch et al., 1999, 2001; Fölsch, 2005). Other such adaptors must exist, as AP-1B does not recognize dileucine signals nor is expressed in all epithelia or polarized cells.

Apical targeting signals are less well defined. Some apical proteins have membrane-anchoring domains that partition into glycolipid raft microdomains; apical targeting often correlates with raft association (Ikonen and Simons, 1998; Rodriguez-Boulan and Gonzalez, 1999). Other apical proteins contain N- or O-linked oligosaccharides in their extracellular domains that may interact with an unidentified lectin that specifies apical transport (Scheiffele et al., 1995; Gut et al., 1998). These apical targeting signals function only in the absence of an active basolateral signal (Matter and Mellman, 1994).

E. Anderson and S. Maday contributed equally to this paper.

Correspondence to Ira Mellman: ira.mellman@yale.edu

E. Anderson's present address is HistoRx, Inc., New Haven, CT 06511.

B. Winckler's present address is Dept. of Neuroscience, University of Virginia Medical School, Charlottesville, VA 22908.

D. Sheff's present address is Dept. of Pharmacology, Carver College of Medicine, University of Iowa, Iowa City, IA 522423.

H. Fölsch's present address is Dept. of Biochemistry, Molecular Biology, and Cell Biology, Northwestern University, Evanston, IL 60208.

Abbreviations used in this paper: abd, ankyrin binding domain; ERM, ezrin-radixin-moesin; grr, glycine-rich region; LDLR, low density lipoprotein receptor; plg-R, polymeric Ig receptor; prr, proline-rich region; shRNA, short hairpin RNA.

The Journal of Cell Biology, Vol. 170, No. 4, August 15, 2005 595–605
http://www.jcb.org/cgi/doi/10.1083/jcb.200506051

Certain membrane proteins in polarized cells undergo transcytosis, moving from one cell surface domain to the other (Tuma and Hubbard, 2003). This mechanism has been proposed for some apical raft proteins (Polishchuk et al., 2004). However, the best-studied transcytotic protein is the polymeric Ig receptor (pIg-R), which transports IgM and dimeric IgA from the basolateral to the apical surface of epithelia (Mostov et al., 2000). The initial basolateral insertion of the pIg-R is mediated by a basolateral targeting signal contained within a 17–amino acid sequence in the receptor's cytoplasmic tail (Casanova et al., 1991; Aroeti et al., 1993; Reich et al., 1996). After basolateral insertion, the pIg-R is internalized and transported to the apical domain in a process stimulated by the presence of bound immunoglobulin (Hirt et al., 1993; Song et al., 1994). Transcytosis is made more efficient by serine phosphorylation of its cytoplasmic tail (Casanova et al., 1990; Okamoto et al., 1994; Luton et al., 1998) and also by the src family tyrosine kinase $p62^{yes}$ (Luton et al., 1999). How $p62^{yes}$ drives pIg-R transcytosis is unknown and may reflect signal transduction events that may be associated with immunoglobulin binding (Mostov et al., 2000); $p62^{yes}$ does not phosphorylate the receptor itself. Further, the mammalian retromer has also recently been shown to promote pIg-R transcytosis, although the mechanism remains unclear (Verges et al., 2004). Indeed, despite considerable progress, a clear understanding of the pIg-R transcytotic mechanism remains elusive.

Given the potential relationship between the mechanisms of sorting among different types of polarized cells, it is of interest to characterize the transport of membrane proteins expressed endogenously by both epithelial cells and neurons. One such protein is NgCAM, a cell adhesion molecule and member of the Ig gene superfamily and chick homologue of human L1 cell adhesion molecule (Walsh and Doherty, 1997; Hortsch, 2000). NgCAM is axonal in neurons (Vogt et al., 1996; Winckler et al., 1999) but is found in variable locations in vivo in epithelial cells (Nolte et al., 1999; Jenkins et al., 2001). Its cytoplasmic domain contains a YXXΦ endocytosis signal and an ankyrin binding domain (abd). Both motifs are regulated by tyrosine phosphorylation (Tuvia et al., 1997; Schaefer et al., 2002). In neurons, NgCAM reaches the axonal plasma membrane after insertion into the somatodendritic domain (Wisco et al., 2003). In MDCK cells, we find NgCAM is also transcytosed and show that transcytosis likely reflects spatial regulation of the NgCAM basolateral targeting signal by a src family kinase. Thus, for at least some proteins, transcytosis may reflect a relatively simple mechanism.

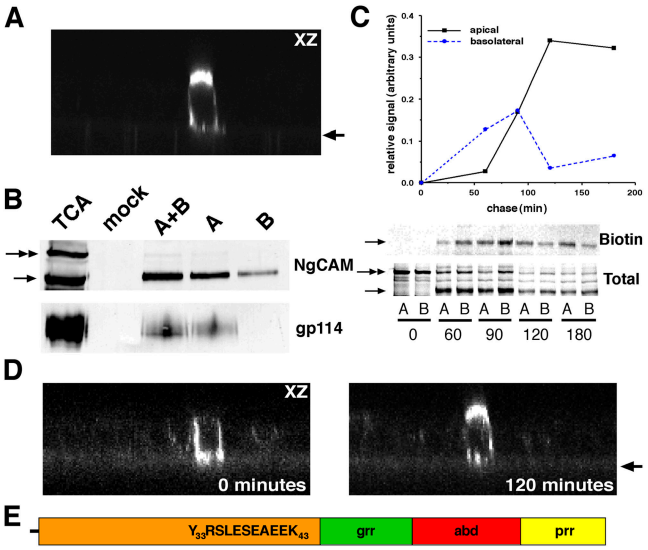

Figure 1. **Localization and trafficking of NgCAM.** (A) Polarized MDCK cells on Transwell filters were microinjected with NgCAM cDNA and incubated at 37°C for 4 h. The cells were then surface stained with the NgCAM-specific mAb 8D9 and processed for immunofluorescence. The cells were then analyzed by confocal microscopy and a representative x-z section is shown. The arrow denotes the position of the filter. (B) Polarized MDCK cells were infected 16 h with AdNgCAM, placed on ice, and either the apical (A), basolateral, (B) or both (A+B) sides biotinylated. TCA precipitations and mock biotinylations were performed as controls. Biotinylated material was immunoblotted with either pAb G4 (NgCAM) or mAb Y652 (gp114). The 210-kD NgCAM precursor is indicated with a double arrow and the mature 135-kD molecule with a single arrow. Identical results were obtained for the 80-kD fragment, which remains complexed to the 135-kD fragment in a 1:1 ratio (not depicted). (C) Polarized MDCK cells were infected 16 h with AdNgCAM, pulse-labeled with [^{35}S]Met/Cys for 15 min, and chased at 37°C. The cells were then biotinylated on either the apical (A) or basolateral (B) surfaces. NgCAM was immunoprecipitated, and the antibody complexes were brought down with protein G–Sepharose beads. The immunoprecipitated material was boiled off the beads and 20% of the total protein was set aside (Total). The remaining material was applied to NeutrAvidin beads. After binding, the beads were spun down and resuspended in SDS-PAGE sample buffer (Biotin). All samples were then subjected to SDS-PAGE and quantitative autoradiography was performed. The strength of the "Biotin" signal was quantitated and normalized to the "Total" signal, adjusting for the relative inputs. (D) Polarized MDCK cells were infected 16 h with AdNgCAM and conditioned hybridoma supernatant containing mAb 8D9 was added to the basolateral chamber. After 30 min at 37°C, the cells were either fixed (0 min) or growth medium was added and the cells were incubated at 37°C for 120 min and then fixed. The arrow denotes the position of the filter. (E) Schematic of the 114-aa cytoplasmic tail of NgCAM. Note that in all constructs, numbering is from the first residue of the cytoplasmic tail, Lys_1.

Results

NgCAM is apical in MDCK cells

We expressed NgCAM in filter-grown MDCK cells by cDNA microinjection to determine its polarized localization. By immunofluorescence, NgCAM was mostly at the apical surface, although limited basolateral staining was observed (Fig. 1 A).

To examine this distribution quantitatively, we infected MDCK cells with recombinant adenovirus-encoding NgCAM, followed by selective biotinylation of either the apical or basolateral surfaces. NgCAM is initially produced as a 210-kD precursor that is endoproteolytically cleaved within its third fibronectin repeat to generate two fragments, a membrane anchored 80-kD fragment and the noncovalently associated 135-kD fragment (Burgoon et al., 1991). All three proteins were visible by Western blot using whole cell lysates, although for simplicity we have only shown the 210- and 135-kD forms (Fig. 1 B). Only the 135- and 80-kD fragments were accessible to biotinylation, consistent with intracellular processing of the 210-kD precursor. As illustrated for the 135-kD fragment, most of the biotinylated NgCAM (~75%) was detected at the apical domain with the remainder found on the basolateral domain (Fig. 1 B). To ensure that virus expression of NgCAM did not

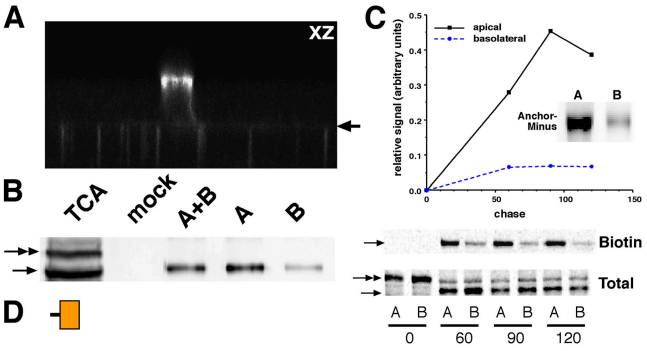

Figure 2. **Localization and trafficking of CT3.** (A) Polarized MDCK cells were microinjected with CT3 cDNA and processed as described in Fig. 1 A. The arrow denotes the position of the filter. (B) Polarized MDCK cells were infected 16 h with AdCT3 and subjected to vectorial biotinylation as described in Fig. 1 B. (C) Pulse-chase biotinylation analysis of CT3 trafficking was performed as described in Fig. 1 C. (inset) The lumenal domain of NgCAM contains a cryptic apical targeting signal. Polarized MDCK cells grown on 24-mm Transwell filters were infected overnight with AdAnchor-Minus. The medium from either the apical or basolateral chambers was then harvested and NgCAM was immunoprecipitated with mAb 8D9. Western blotting for NgCAM was performed with pAb G4. (D) Schematic of the 3-aa cytoplasmic tail of CT3.

affect the overall organization of the infected cells, we monitored the distribution of the endogenous apical marker gp114. By surface biotinylation, gp114 was apically polarized to an even greater extent (>90%).

NgCAM undergoes basolateral to apical transcytosis

The presence of a significant fraction of basolateral NgCAM suggested that at least a portion of the protein might reach the apical surface by transcytosis. We thus performed a pulse-chase radiolabeling experiment in which a cohort of NgCAM was followed by vectorial biotinylation (for review see Matter et al., 1992). After a 15-min pulse in ^{35}S-methionine/cysteine, adenovirus-infected MDCK cells expressing NgCAM were chased in unlabeled medium. At various chase times, the filter-grown cells were placed on ice, the apical or basolateral surfaces were biotinylated, and labeled/biotinylated NgCAM was detected by immunoprecipitation using an anti-NgCAM monoclonal antibody followed by capture on NeutrAvidin linked to polyacrylamide beads.

Labeled NgCAM appeared first at the basolateral surface after 60 min of chase; little labeled protein was recovered from the apical surface (Fig. 1 C). Although basolateral NgCAM increased slightly between 60 and 90 min, it decreased rapidly thereafter. In contrast, beginning at 90 min, apical NgCAM increased dramatically, reaching a plateau by 120 min. This transient appearance at the basolateral surface followed by accumulation at the apical surface suggested that newly synthesized NgCAM reached the apical surface indirectly, i.e., by transcytosis. Transcytosis was further demonstrated by the fact that anti-NgCAM antibody added to the basolateral medium was transcytosed to the apical surface (Fig. 1 D). Simultaneous uptake of mAb 8D9 and fluorescently labeled transferrin in live cells suggested that NgCAM passes through perinuclear recycling endosomes during transport to the apical surface (unpublished data).

NgCAM transcytosis involves cytoplasmic and extracellular domain signals

We speculated that transcytosis might involve interplay between conventional basolateral and apical targeting signals. Thus, we expressed a COOH-terminal truncation mutant lacking all but the first three amino acids of the cytoplasmic tail (CT3; Fig. 2 D). Like native NgCAM, CT3 was mostly apical at steady state when assayed by immunofluorescence or by vectorial biotinylation and Western blotting (Fig. 2, A and B). However, analysis of its delivery pathway by pulse-chase biotinylation revealed that CT3 was directly inserted into the apical domain (Fig. 2 C). Thus, the NgCAM cytoplasmic tail was necessary for transcytosis.

Apical as opposed to random insertion of CT3 suggested the existence of apical sorting information in the transmembrane and/or lumenal domains. Thus, we generated "Anchor-Minus" NgCAM, in which a stop codon was inserted just before the transmembrane domain. Anchor-Minus was expressed overnight in polarized MDCK cells, the apical and basolateral medium was harvested, and NgCAM was immunoprecipitated. Western blot analysis revealed that Anchor-Minus was predominantly secreted into the apical medium (Fig. 2 C, inset). Thus, the lumenal domain of NgCAM contains a cryptic apical sorting signal.

The distal cytoplasmic domain is necessary for transcytosis

To better understand the role of NgCAM's cytoplasmic tail in mediating transcytosis, we fine-tuned our truncation analysis. Previous work demonstrated that the NgCAM tail contains multiple domains that might affect polarized transport, including a putative actin-binding element ($KGGK_7$; Dahlin-Huppe et al., 1997) that may be an ezrin-radixin-moesin (ERM)–binding site (Cheng et al., 2005), an internalization motif ($Y_{33}RSL$) known to bind the AP-2 clathrin adaptor (Kamiguchi et al., 1998; Schaefer et al., 2002), another ERM-binding site (Dickson et al., 2002), the conserved abd Ser_{65}-Tyr_{92} (Davis et al., 1993), and the 23-residue proline-rich region (prr) Arg_{93}-Asp_{114} (26% proline residues). The endocytosis motif is followed by a cluster of charged residues ($Y_{33}RSLESEAEEK_{43}$) and then the 23-residue glycine-rich region (grr) Gly_{44}-Gly_{66} (39% glycine residues). The charged cluster might be associated with the endocytosis motif, perhaps contributing to basolateral targeting, as found for the low density lipoprotein receptor (LDLR; for review see Matter et al., 1992). Further, the grr might be a flexible linker dividing the tail into two functional domains, separating the actin binding, endocytosis, and ERM binding motifs from the abd and prr. Thus, we truncated the cytoplasmic tail just before the grr to generate CT43 (Fig. 3 E).

This truncation had a dramatic effect on NgCAM localization. At steady state, CT43 was predominantly basolateral (Fig. 3, A and B). Pulse-chase biotinylation of cells infected with a recombinant adenovirus encoding CT43 revealed that this mutant inserted directly into the basolateral surface and did not undergo transcytosis (Fig. 3 C). Further, anti-NgCAM antibody added to the basolateral surface of adenovirus-infected

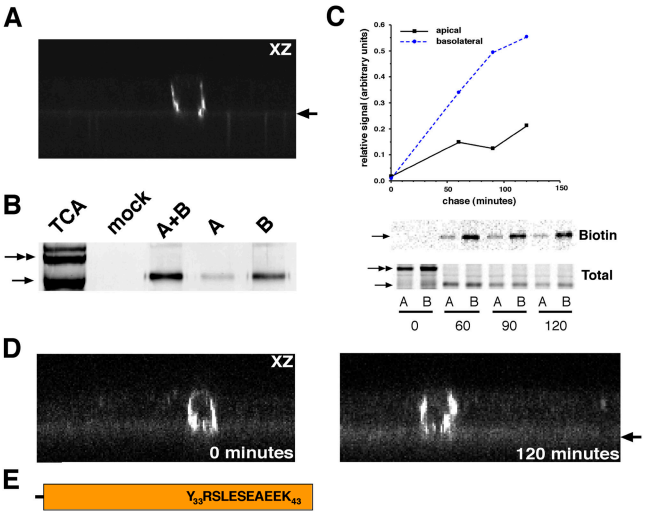

Figure 3. **Localization and trafficking of CT43.** (A) Polarized MDCK cells were microinjected with cDNA encoding CT43 and processed as described in Fig. 1 A. The arrow denotes the position of the filter. (B) Polarized MDCK cells were infected overnight with AdCT43 and subjected to vectorial biotinylation as described in Fig. 1 B. (C) Pulse-chase biotinylation analysis of CT43 trafficking was performed as described in Fig. 1C. (D) Antibody uptake analysis was performed as in Fig. 1 D. The arrow denotes the position of the filter. (E) Schematic of the 43-aa cytoplasmic tail of CT43.

MDCK cells was not transcytosed to the apical surface (Fig. 3 D). Thus, the distal portion of the cytoplasmic tail is required for transcytosis, despite the apical targeting signal in the NgCAM extracellular domain.

Basolateral sorting of CT43 is controlled by Tyr_{33}

Because many basolateral targeting signals include critical tyrosine residues, we asked if the Y_{33}RSL motif served this function in NgCAM. We disrupted this motif by mutating Tyr_{33} to Ala in the context of the CT43 construct to generate CT43(Y33A). CT43(Y33A) was predominantly apical in MDCK cells (Fig. 4 A), and pulse-chase biotinylation experiments confirmed that it was directly inserted into the apical domain (not depicted).

To demonstrate that the Y_{33}RSL motif was responsible for initial basolateral delivery of full-length NgCAM, we mutated Tyr_{33} to Ala in the context of the native molecule to generate NgCAM(Y33A). NgCAM(Y33A) was apical at steady state (Fig. 5, A and B) and inserted directly into the apical domain (Fig. 5 C). Thus, Tyr_{33} is critical for the initial sorting of NgCAM to the basolateral surface of MDCK cells.

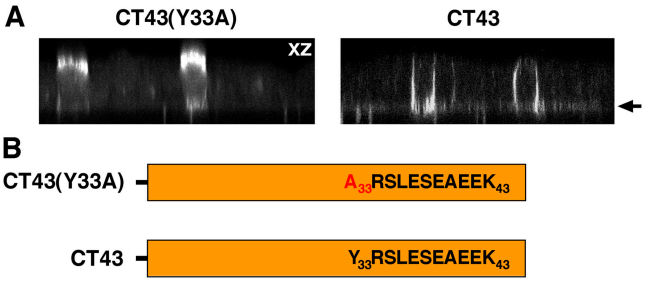

Figure 4. **NgCAM contains a tyrosine-based basolateral sorting signal.** (A) Polarized MDCK cells were microinjected with cDNA encoding either CT43(Y33A) or CT43. The cells were then processed as described in Fig. 1 A. The arrow denotes the position of the filter. (B) Schematics of the CT43(Y33A) and CT43 cytoplasmic tails.

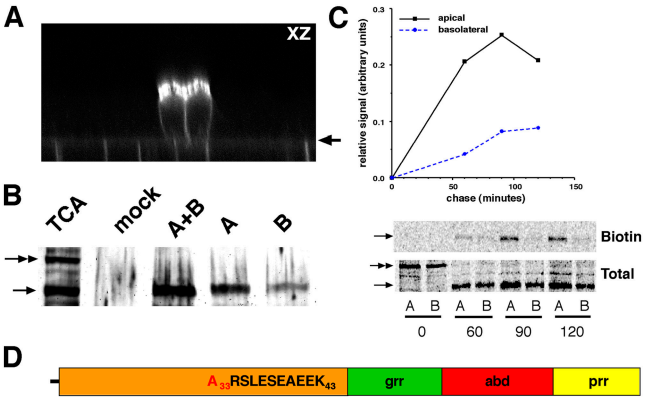

Figure 5. **Localization and trafficking of NgCAM(Y33A).** (A) Polarized MDCK cells were microinjected with the cDNA encoding NgCAM(Y33A) and processed as described in Fig. 1 A. The arrow denotes the position of the filter. (B) Polarized MDCK cells were infected overnight with AdNgCAM(Y33A) and subjected to vectorial biotinylation as described in Fig. 1 B. (C) Pulse-chase biotinylation analysis was performed as described in Fig. 1 C. (D) Schematic of the 114-aa cytoplasmic tail of NgCAM(Y33A).

AP-1B mediates the basolateral insertion of NgCAM

Next, we analyzed whether the epithelial cell-specific adaptor complex AP-1B plays a role in the polarized transport of NgCAM. For this purpose, we used LLC-PK1 pig kidney epithelial cells, which do not express the μ1B subunit of the AP-1B complex (Ohno et al., 1999), and, as a result, basolateral proteins that require AP-1B for sorting are either apical or unpolarized (Roush et al., 1998; Fölsch et al., 1999, 2001). Two stable cell lines were generated from the LLC-PK1 parent: LLC-PK1::μ1A and LLC-PK1::μ1B, exogenously expressing μ1A and μ1B, respectively. Previous work from our laboratory demonstrated that exogenous expression of μ1B but not the ubiquitously expressed μ1A rescued the sorting phenotype (Fölsch et al., 1999). As shown in Fig. 6 A, native NgCAM was apical in both cell lines. In contrast, the CT43 mutant was apical in LLC-PK1::μ1A cells and basolateral in LLC-PK1::μ1B cells, as found for the AP-1B–dependent basolateral protein LDLR (Fig. 6 A). Thus, CT43 requires AP-1B for basolateral sorting. Because LLC-PK1 cells do not form tight monolayers, it was impossible to perform pulse-chase biotinylation experiments (Fölsch et al., 1999), so we were unable to determine if native NgCAM reached the apical surface via transcytosis.

To demonstrate conclusively the role of AP-1B in the sorting of NgCAM, we next performed a loss-of-function experiment by a stable knockdown of μ1B in MDCK cells through the use of RNA interference (Elbashir et al., 2001). We generated a recombinant retrovirus encoding a short hairpin RNA (shRNA) specifically designed to MDCK μ1B, infected MDCK cells, and selected for stable clones (Barton and Medzhitov, 2002; Brummelkamp et al., 2002; Schuck et al., 2004). Using whole cell lysates, quantitative Western blotting

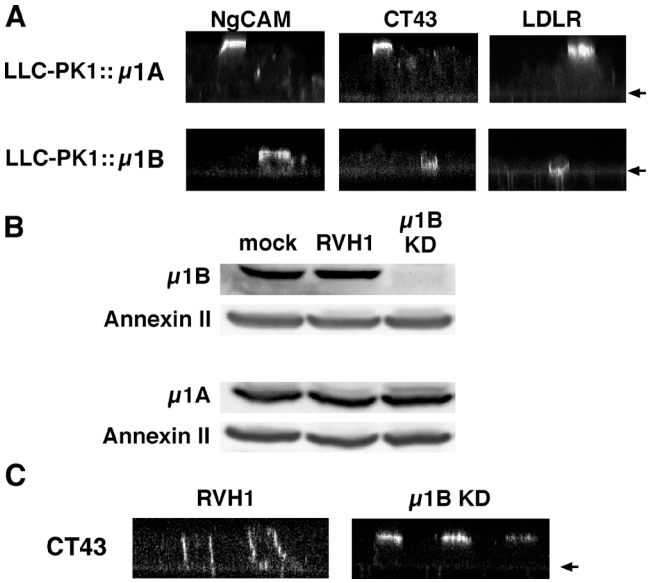

Figure 6. **NgCAM interacts with AP-1B.** (A) Polarized LLC-PK1::μ1A or LLC-PK1::μ1B cells were infected with either AdNgCAM, AdCT43, or AdLDLR. After overnight incubation at 37°C, the cells were surface stained with mAb 8D9 (NgCAM) or mAb C7 (LDLR) and fixed and processed for immunofluorescence. Confocal microscopy was performed and representative x-z sections are shown. The arrows denote the position of the filters. (B) MDCK cells were either mock infected or infected with RVH1 empty virus or RVH1 encoding an shRNA directed against μ1B. Equal amounts of whole cell lysates were immunoblotted for μ1B, μ1A, or annexin II. (C) Polarized RVH1 empty virus and μ1B knockdown cells were infected with AdCT43. After overnight incubation at 37°C, the cells were surface labeled with mAb 8D9, fixed and processed for immunofluorescence, and analyzed by confocal microscopy. The arrow denotes the position of the filter.

revealed that we are able to knockdown the expression of μ1B in MDCK cells by >99%, as compared with the empty virus vector and mock-infected cells (Fig. 6 B); the degree of knockdown was quantified by serial dilution of MDCK cell lysates followed by Western blot (not depicted). Knockdown of μ1B was also specific, as the level of μ1A expression remained unaffected. The lysates were also probed for annexin II as a control for equal loading; annexin II expression was also unaffected by the μ1B shRNA virus.

As shown in Fig. 6 C, CT43 was predominantly basolateral in the RVH1 empty virus control cells, indicating that the polarity of the cells was not disrupted by retroviral infection. When the level of μ1B expression was knocked down, however, CT43 was mislocalized to the apical membrane in nearly all of the NgCAM-expressing cells. The missorting phenotype was reproduced with an shRNA designed to another region within the μ1B sequence, confirming the specificity of the effect. In general, the μ1B knockdown affected the polarized expression only of proteins found previously to be sorted to the basolateral surface by AP-1B (unpublished data). Combined with the LLC-PK1 gain-of-function experiment (Fig. 6 A), the loss of basolateral polarity after μ1B knockdown demonstrates that CT43 requires AP-1B for sorting to the basolateral surface. This, in turn, is likely to reflect the adaptor's recognition of Tyr33 in the NgCAM cytoplasmic domain, which defines the single motif required for basolateral targeting.

Phosphorylation of Tyr_{33} and the regulation of NgCAM transcytosis

A simple model for how NgCAM undergoes transcytosis would involve (a) AP-1B–dependent sorting after exit from TGN, (b) subsequent inactivation of the tyrosine-based basolateral sorting signal to prevent basolateral recycling from endosomes (Matter et al., 1993; Aroeti and Mostov, 1994), and (c) sorting to the apical surface mediated by cryptic sorting information within the lumenal domain. Schaefer et al. (2002) found that p60src phosphorylates the L1/NgCAM YRSL motif, a modification that interferes with AP-2 binding in vitro, presumably slowing endocytosis in vivo. We reasoned that phosphorylation of Tyr_{33} might also inhibit AP-1B binding and thus prevent basolateral recycling from endosomes.

We first tested if in vivo tyrosine kinase activity is required for the apical localization of NgCAM. MDCK cells were infected overnight with an adenovirus encoding native NgCAM and incubated for 5 h in medium containing the tyrosine kinase inhibitor herbimycin A. Strikingly, this treatment resulted in a predominantly basolateral localization of NgCAM (Fig. 7 A). In contrast, the apical CT3 and basolateral CT43 constructs were unaffected. The endogenous basolateral marker gp58 was also unaffected (unpublished data). At least qualitatively, herbimycin A treatment did not block endocyto-

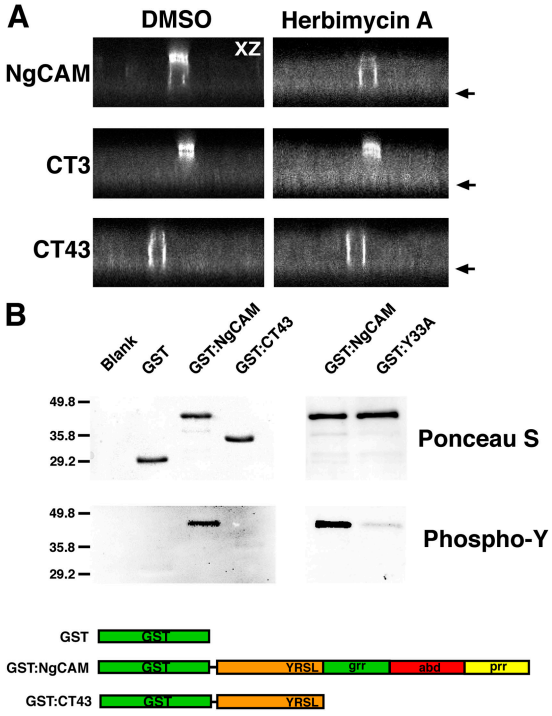

Figure 7. **The potential role of tyrosine phosphorylation in NgCAM transcytosis.** (A) Polarized MDCK cells infected 16 h with either AdNgCAM, AdCT3, or AdCT43 were treated for 5 h with 12.5 μg/ml herbimycin A or DMSO as a control. Representative confocal x-z sections are shown. The arrows denote the position of the filters. (B) The indicated GST fusion proteins were incubated with purified his-p60src in the presence of ATP. After incubation, the samples were subjected to SDS-PAGE and transferred to nitrocellulose, which was Ponceau S stained (top) and then immunostained with an antiphosphotyrosine pAb (bottom). Blank, a control sample containing no added GST protein. Molecular mass markers (labeled in kD) migrated as indicated.

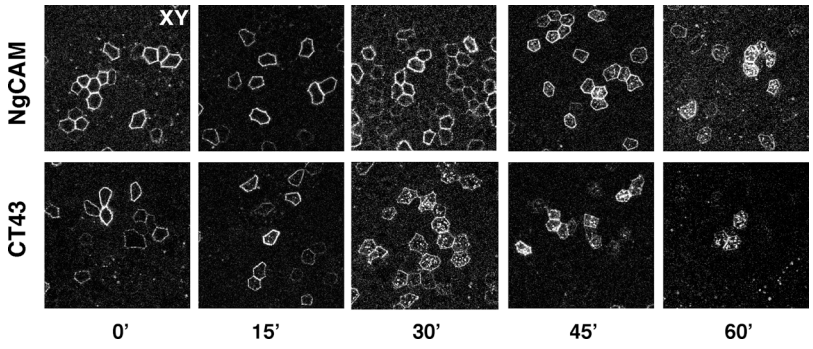

Figure 8. **Endocytosis of native NgCAM and CT43 from the basolateral surface.** MDCK cells infected 16 h with either AdNgCAM or AdCT43 were stained on the basolateral surface for NgCAM with mAb 8D9. The cells were then refed with growth medium and returned to the 37°C incubator for 0, 15, 30, 45, 60, or 90 min, and then processed for immunofluorescence.

sis of wild-type NgCAM or CT43 as indicated by the internalization of NgCAM-specific monoclonal antibodies by live cell imaging (unpublished data). These data suggest that herbimycin A inhibits transcytosis at least in part by blocking the apical sorting of internalized NgCAM.

Because herbimycin A acts to block the activity of src family kinases, we speculated that p60src activity might be responsible for the dramatic difference in the polarized traffic of NgCAM and the CT43 mutant. Unfortunately, due to its lability, it has proven technically difficult for us or others (Schaefer et al., 2002) to study the phosphorylation of Tyr_{33} of NgCAM directly in cell lines (see Discussion). Therefore, to determine if native NgCAM and CT43 were differentially susceptible to phosphorylation by p60src, we generated GST fusion proteins representing the full-length NgCAM cytoplasmic tail (GST:NgCAM) and the CT43 cytoplasmic tail (GST:CT43). These constructs were incubated with purified his-tagged p60src and ATP. As shown in Fig. 7 B, GST:NgCAM was efficiently phosphorylated in vitro, as found previously (Schaefer et al., 2002). However, GST:CT43 was not a substrate for p60src. This result was striking given that Tyr_{33} was confirmed as the site of phosphorylation in the full-length cytoplasmic tail because GST:NgCAM(Y33A) was not phosphorylated by his-p60src (Fig. 7 B). We suspect that GST:CT43 was not phosphorylated due to the fact that it lacked the prr that contains a cryptic SH3 domain possibly required for p60src recruitment. Regardless of the mechanism, however, these results suggest that phosphorylation of the critical tyrosine in the Y_{33}RSL motif by p60src or a related tyrosine kinase acts as a regulator of AP-1B–mediated sorting of NgCAM to the basolateral domain.

As further evidence of the NgCAM phosphorylation state in vivo, we examined the basolateral uptake of anti-NgCAM antibodies by MDCK cells expressing either native NgCAM or CT43. Even using a qualitative immunofluorescence assay, it was evident that wild-type NgCAM mediated antibody endocytosis far more slowly than CT43. Intracellular antibody was detected in CT43-expressing cells within 15–30 min after warming to 37°C, whereas at least 45 min was required in the case of wild-type–expressing cells (Fig. 8). These data are consistent with the idea that Tyr_{33} in wild-type NgCAM was phosphorylated at the basolateral surface, and therefore less able to interact with AP-2 adaptors than the more rapidly internalized, nonphosphorylatable mutant CT43. Because AP-2 interacts with the same tyrosine residue required for AP-1B–dependent sorting, it is reasonable to presume that basolateral targeting from endosomes would similarly be impaired.

Discussion

Despite nearly two decades of excellent work, an understanding of the mechanisms enabling transcytosis in epithelial cells has remained elusive. Previous efforts have also not placed this process in the context of adaptor complexes such as AP-1B in polarized transport. Fundamental principles were established by the efforts of Mostov et al. working on pIg-R (for review see Mostov et al., 2000). For example, it has long been clear that newly synthesized pIg-R reaches the basolateral domain by virtue of targeting information in its cytoplasmic tail (Mostov and Deitcher, 1986; Casanova et al., 1991). In addition, transcytosis of the receptor to the apical surface was clearly established as reflecting polarized sorting in endosomes (Apodaca et al., 1994; Barroso and Sztul, 1994). However, several basic mechanistic issues remain unclear. A variety of factors contribute separately or together to pIg-R transcytosis, perhaps because the receptor itself has been associated with various signal transduction events (Singer and Mostov, 1998). Binding dimeric IgA enhances the basal rate of transcytosis, although it is unclear if this acts by silencing the basolateral targeting signal or by activating an apical targeting signal. Phosphorylation of Ser_{664} has been implicated, although it is not essential and outside of the region required for basolateral targeting. Most relevant to our consideration, transcytosis of pIg-R is regulated directly or indirectly by $p62^{yes}$ (Luton et al., 1999). $p62^{yes}$ can be coprecipitated with the receptor, and $p62^{yes}$ $-/-$ mice are less capable of transporting dIgA into the bile than wild-type mice. However, pIg-R is not a substrate for $p62^{yes}$, nor is it clear how or why $p62^{yes}$ is involved in this pathway.

We have characterized in detail NgCAM as another transcytotic protein in MDCK cells. In the process, we obtained evidence that NgCAM's circuitous route from the TGN to the apical domain can be explained by a spatially regulated interplay of well-known signals for basolateral versus apical transport. Although several elements of the model remain to be tested, it seems likely that NgCAM is targeted from the TGN to the basolateral surface as an AP-1B–dependent cargo molecule. Its Y_{33}RSL basolateral targeting motif is then inactivated by phosphorylation, likely preventing it from interacting with AP-1B or a functionally equivalent adaptor in endosomes. Consequently, phosphorylated NgCAM would not be recycled

to the basolateral surface but rather be transported to the apical domain via its cryptic apical targeting signal.

In vivo phosphorylation of Tyr_{33}

Our data suggest that phosphorylation of Tyr_{33} by a src family member facilitates the transcytosis of NgCAM. This conclusion must be tempered by the fact that we have been unable to demonstrate directly where in the cell NgCAM is phosphorylated. Our attempts to use a relevant phosphospecific antibody (Schaefer et al., 2002) were unsuccessful due to cross-reactivity with endogenous MDCK proteins (unpublished data). Further, direct examination of the Tyr_{33} phosphorylation state in vivo using radiolabeling or phosphotyrosine-specific antibodies was made difficult by the numerous phosphorylated residues in the NgCAM cytoplasmic tail, including a second tyrosine (Tuvia et al., 1997). Additionally, the phosphate moiety on Tyr_{33} has been found to be difficult to stabilize after cell lysis (unpublished data); indeed, phosphorylated NgCAM has only been studied biochemically in primary tissues, using much larger quantities of material than possible in cell culture (Schaefer et al., 2002).

In light of these problems, we generated a panel of GST fusion proteins and examined their ability to be phosphorylated with purified his-p60src. Our in vitro findings were consistent with differential phosphorylation states being responsible for the in vivo trafficking of the corresponding NgCAM constructs. This idea was further supported by our finding that herbimycin A selectively causes NgCAM to mislocalize. Herbimycin A inhibits a wide range of src family kinases in vivo by triggering their degradation (Whitesell et al., 1994).

The simplest view would be that Tyr_{33} phosphorylation occurs at some point after exit of newly synthesized NgCAM from the sites at which polarized sorting occurs in the secretory pathway and before its arrival in endosomes after internalization from the basolateral surface. This necessity is emphasized by our recent observation that both endocytic and biosynthetic sorting in MDCK cells may occur at a single site, recycling endosomes (Ang et al., 2004). Because active src has been localized to the plasma membrane of many cells, it seems most likely that this is the site at which NgCAM is phosphorylated. Consistent with this possibility is the fact that NgCAM is internalized relatively slowly from the plasma membrane, certainly relative to the rate of CT43 whose Tyr_{33} is not subject to phosphorylation (at least in vitro). Src-mediated phosphorylation of Tyr_{33} would be expected to slow endocytosis because this modification interferes with interaction with the endocytic clathrin adaptor AP-2 via the Y_{33}RSL motif (Schaefer et al., 2002). Thus, the relatively slow endocytosis of native NgCAM from the basolateral surface is consistent with its having been phosphorylated at or just before plasma membrane arrival, although transient association with a basolateral ankyrin isoform via the NgCAM abd cannot be ruled out. Presumably, phosphorylation earlier in the secretory pathway would have similarly disrupted its ability to interact with AP-1B or a related adaptor required for initial basolateral targeting. This would lead to direct apical targeting of new molecules, as occurred when the targeting signal was inactivated by mutagenesis (e.g., NgCAM [Y33A]).

In any event, we propose that NgCAM phosphorylation is spatially regulated such that a common signal for polarized sorting is "on" within the biosynthetic route and "off" within the endocytic route. As discussed in the previous paragraph, this asymmetry may reflect the restricted intracellular distribution of the relevant src family kinase responsible for the modification. On the other hand, it is also possible that the kinase is widely distributed and phosphorylation is spatially restricted due to conformational changes in NgCAM itself. It is possible that such conformational changes may involve interaction with ankyrin family members. We speculate that a src family kinase interacts with the prr, perhaps via this domain's potential SH3 binding site ($PASP_{107}$). Because the prr and abd are next to each other in the primary sequence (Fig. 1 E), kinase and ankyrin binding may be mutually exclusive due to steric hindrance. Thus, a Golgi-associated ankyrin might prevent phosphorylation of Tyr_{33} at the level of the TGN. Because our CT43 truncation removed both the prr and the abd, their individual contributions will need to be analyzed in future work. Preliminary experiments revealed that selective deletion of the abd results in direct transport of NgCAM to the apical surface, and selective deletion of the prr results in direct transport to the basolateral surface (unpublished data). These finding are consistent with a conformational or allosteric mechanism regulating kinase interaction.

Sorting of NgCAM in neurons versus epithelial cells

Our recent work demonstrated that NgCAM undergoes somatodendritic to axonal transcytosis in neurons (Wisco et al., 2003). In contrast, another recent study concluded that selective vesicle fusion was responsible for NgCAM's axonal delivery (Sampo et al., 2003). Although it is possible that neurons and epithelial cells have different mechanisms governing the traffic of NgCAM, our current study provides additional support for a transcytotic mechanism in neurons. This, in turn, supports the general view that there are strong similarities between polarized transport in these two cell types, at least with respect to shared reliance on basolateral (somatodendritic) targeting signals (for review see Winckler and Mellman, 1999). However, some proteins, especially GPI-anchored "raft proteins," that are apical in epithelial cells may not be as strongly polarized to the axonal domain in neurons (Jareb and Banker, 1998; Winckler et al., 1999). It may be that although axonal targeting signals are decoded as apical signals in epithelial cells, the reverse is not necessarily true. Indeed, it is possible that raft proteins are not sorted from basolateral proteins in the biosynthetic pathway (Polishchuk et al., 2004).

Another key difference between the sorting mechanism in epithelial cells and neurons is the differential expression of μ1B. Given the likely role played by AP-1B in NgCAM sorting in epithelial cells, there must be equivalent molecules fulfilling this role in neurons. Several possibilities are suggested by studies on AP-4 (Simmen et al., 1999), doublecortin (Kizhatil et al., 2002), and ERM family members (Dickson et al., 2002). It may be that interaction with one or more of these components functionally fulfills the role of AP-1B.

In vivo role of transcytosis

A recent study has presented evidence that glycolipid raft–associated proteins may undergo transcytosis in epithelial cells (Polishchuk et al., 2004), although the physiological significance of this trafficking pattern is unclear. Because most NgCAM does not partition into lipid rafts (Kleene et al., 2001), we do not expect that this mechanism plays a role.

The pIg-R is the only other molecule directly demonstrated to undergo transcytosis in epithelial cells (for review see Mostov et al., 2000). Although a physiologically significant role for pIg-R transcytosis is readily apparent (secretion of IgA and IgM to confer mucosal immunity), it is unclear why NgCAM reaches the apical plasma membrane by such a circuitous route.

In vivo, NgCAM not only mediates cell adhesion but also plays an important role in intracellular signaling (for reviews see Peles et al., 1998; Doherty et al., 2000; Kamiguchi and Lemmon, 2000). Given these intertwined roles, it is possible that transient somatodendritic localization allows NgCAM to find spatially polarized binding partners. Interestingly, local somatodendritic interactions with NgCAM influence the choice of axonal extension substrate (Esch et al., 1999). Another possibility is that NgCAM transcytosis facilitates interaction with signal transduction molecules located throughout the cell. Indeed, NgCAM interacts, directly or indirectly, with numerous intracellular and extracellular binding partners; e.g., $p90^{rsk}$ (Wong et al., 1996), ERK2 (Schaefer et al., 1999), integrins (Felding-Habermann et al., 1997; Silletti et al., 2000), and ERM family members (Dickson et al., 2002). Further in vivo analysis will be required to determine the reason for NgCAM's unusual intracellular itinerary.

Materials and methods

Antibodies and reagents

The 8D9 hybridoma expressing mouse anti-NgCAM IgG was obtained from the Developmental Studies Hybridoma Bank (University of Iowa). The C7, Y652, and 6.23.3 hybridomas expressing mouse anti-human LDLR, anti-gp114, and anti-gp58 IgGs, respectively, were obtained from the American Type Culture Collection. The goat anti-NgCAM polyclonal antibody G4 was provided by P. Sonderegger (University of Zurich, Zurich, Switzerland). Rabbit antiphosphotyrosine antibody was purchased from Upstate Biotechnology. AP- and HRP-conjugated secondary antibodies were purchased from Pierce Chemical Co. Alexa 488–conjugated goat anti–mouse antibody was obtained from Molecular Probes. Herbimycin A was obtained from Calbiochem, and the stock solution was prepared in DMSO. All other reagents were purchased from Sigma-Aldrich unless otherwise indicated.

Cell culture

MDCK cells were maintained in MEM (Invitrogen) supplemented with 10% FBS (vol/vol; Invitrogen) and 2 mM L-glutamine. Stably transfected LLC-PK1 cells were maintained in α-MEM with 10% FBS, 2 mM L-glutamine, and 1.8 mg/ml geneticin (Invitrogen). All cells were maintained at 37°C in a 5% CO_2 incubator.

Generation of constructs and recombinant adenoviruses

NgCAM (variant; GenBank/EMBL/DDBJ accession no. Z75013) cDNA and recombinant adenovirus expressing NgCAM were obtained from P. Sonderegger. The NgCAM gene was amplified by PCR using the oligonucleotides NgC17 and NgC25 (Table I) and cloned into pALTER-MAX (Promega) using the introduced XhoI and XbaI sites. Introduction of stop codons and XbaI sites after Ser_3, Lys_{43}, and Lys_{23} to make CT3, CT43, and Anchor-Minus, respectively, was done using the Altered Sites II kit (Promega) with the indicated oligos (Table I). Introduction of the Tyr_{33} to Ala mutation to generate CT43(Y33A) and NgCAM(Y33A) was performed using the oligo Y33A. The NgCAM constructs were cloned into pShuttleCMV (QBIOGENE) using the introduced XhoI and XbaI sites. Recombinant adenovirus was generated using the AdEasy system (QBIOGENE).

Table I. **Oligonucleotides used for mutagenesis and PCR**

Oligo	Sequence (5′–>3′)
NgC17	CGCG**TCTAGA**TTAATCCAGGGGGGGCCC
NgC25	GCGC**CTCGAG**ATGGCTCTGCCCCATGGG
NgC66	GCGC**CTCGAG**CTAATCCAGGGGGGGCCCAGC
NgC67	GCGC**TCTAGA**CTAATCCAGGGGGGGCCCAGC
NgC68	GCGC**CTCGAG**CTACTTCTCCTCCGCTTCGCTCTC
CT3	GTCCTTCACCGAATACTTGCCCCC**TCTAGA**TTAGC-TGCGTTTGATGAAGCAGAGGATG
CT43	GCCGGAACCCGAAGCCGAACC**TCTAGA**TTACTTC-TCCTCCGCTTCGCTCTCC
Anchor-Minus	GCTGACGAAGCCGATGAACCACCC**TCTAGA**TTAC-TTGGTGGCAAACCCCCCCACCAG
Y33A	CTCCTCCGCTTCGCTCTCCAACGACCTGGCCTCC-CCAAAGGTCTCATCCTTCATGGGCC

Sequences complementary to NgCAM cDNA are underlined and introduced restriction sites are in bold.

Generation of GST fusion proteins

PCR products of the native NgCAM, CT43, or NgCAM(Y33A) cytoplasmic tails were generated with the oligos NgC66, NgC67, and NgC68 using NgCAM or NgCAM(Y33A) cDNA. The amplified gene products were cloned into pGEX6P1 (GE Healthcare) to generate GST:NgCAM, GST:CT43, and GST:NgCAM(Y33A). These plasmids were transformed into BL21-Gold *Escherichia coli* (Stratagene), and fusion proteins were generated using standard procedures. Protein concentrations were determined by Bradford assay.

Biotinylation analysis

To determine the steady-state distribution of NgCAM, MDCK cells were plated on 24-mm polycarbonate Corning-Costar Transwell filters (0.4-μm pore size; Corning, Inc. Life Sciences) at a density of 1.6×10^6 cells and cultured for 4 d. Cells were infected at 14 pfu/cell for 1 h in 250 μl MEM. Cells were then fed with growth medium and incubated at 37°C. 16 h later the cells were placed on ice and subjected to either apical or basolateral biotinylation using 1.6 mg/ml EZ-link sulfo-NHS-LC-LC-biotin (Pierce Chemical Co.) in PBS^{2+} (PBS; 2 g/liter KCl, 2 g/liter KH_2PO_4, 8 g/liter NaCl, and 1.15 g/liter Na_2HPO_4, pH 7.4] plus 147 g/liter $CaCl_2$–2 H_2O, 1 g/liter $MgCl_2$–6 H_2O). After 20 min, the biotinylation reagent was removed, fresh reagent added, and the reactions continued another 20 min. The filters were washed 3× 5 min in 100 mM glycine and 2× 5 min in 20 mM glycine, both in PBS^{2+}. The filters were excised and the cells harvested by scraping into 1.25 ml Harvest $Buffer_1$ (HB_1; 1% Triton X-100, 1× cOmplete Protease Inhibitor Cocktail with EDTA [Roche Diagnostics] and 20 mM glycine in PBS), transferred to microcentrifuge tubes and passaged 4× through 22-gauge needles. The samples were incubated on ice for 30 min and spun at 16,000 *g* for 15 min at 4°C. The supernatant was applied to 100 μl of Ultralink Immobilized NeutrAvidin slurry (Pierce Chemical Co.). After a 1-h incubation at 4°C, the beads were washed 3× in HB_1, once in 2% SDS in PBS, twice in high salt buffer (5 mM EDTA, 350 mM NaCl, and 0.1% TX-100 in PBS), and once in PBS. The beads were then resuspended in 50 μl of 2× SDS-PAGE sample buffer (4% SDS [wt/vol], 20% glycerol [wt/vol], 10% 2-mercaptoethanol [vol/vol], 0.02% bromophenol blue [wt/vol], and 120 mM Tris-HCl, pH 8.0) and 20-μl aliquots were subjected to SDS-PAGE and analyzed by Western blotting with pAb G4 or Y652.

Analysis of NgCAM trafficking kinetics was performed essentially as described for the LDLR (for review see Matter et al., 1992). Cells were infected as described in the previous paragraph, and then starved for 30 min in MEM–Met–Cys (ICN Biomedicals) with 10% dialyzed FBS. Cellular proteins were pulse labeled with 2 mCi/ml [^{35}S]Met/Cys (EXPRE^{35}S^{35}S Protein Labeling mix; PerkinElmer) for 15 min at 37°C. The cells were then chased in growth medium with 5× Met/Cys and biotinylated as described in the previous paragraph. The filters were excised and harvested by scraping into 1.25 ml of Harvest $Buffer_2$ (HB_2; 1% Triton X-100, 1× cOmplete Protease Inhibitor cocktail without EDTA [Roche], 20 mM glycine, 5 mM $MgCl_2$, and 1 mM EGTA in PBS). Cells were then passaged

4× through 22-gauge needles and spun for 15 min at 16,000 *g* at 4°C. The supernatant was then spun at 100,000 *g* for 30 min in an ultracentrifuge (model TLA100; Beckman Coulter). The supernatant was applied to 200 μl of a 50% slurry of protein G–Sepharose beads (Zymed Laboratories) and incubated for 1 h at 4°C. The beads were spun down and the supernatant applied to 8D9-bound protein G–Sepharose beads. Samples were incubated 16 h at 4°C and washed 3× in HB_2 and twice in NET-N (150 mM NaCl, 5 mM EDTA, 0.5% NP-40, 0.01% NaN_3, 0.1% SDS, and 50 mM Tris-HCl, pH 8.0) with vortexing. The beads were then resuspended in 100 μl SDS buffer (100 mM NaCl, 20 mM glycine, 2% SDS, and 20 mM Tris-HCl, pH 8.0), vortexed, boiled for 2 min, and the beads spun down. 20 μl of supernatant was taken for the "Total" sample. The remaining supernatant was mixed with 1 ml of Biotin buffer (1% SDS, 1% TX-100, 20 mM glycine, 1× cOmplete Protease Inhibitor Cocktail with EDTA [Roche] in PBS) and applied to NeutrAvidin slurry and biotinylated material brought down as described above to yield the "Biotin" sample. All samples were subjected to SDS-PAGE and autoradiography. Radioactive counts were detected using a PhosphorImager (model Storm 860; GE Healthcare). The resultant signals were analyzed using IP Lab Gel (Life-Science Software). For quantification, the relative signal obtained from the "Biotin" sample was divided by the signal obtained by the "Total" sample. Results were graphed using Cricket Graph (Computer Associates).

Immunofluorescence

For microinjection, MDCK cells were plated on 12-mm Transwell filters (0.4-μm pore size) at a density of 10^5 cells per filter 4 d before microinjection with a system consisting of a Transjector 55246 and a Micromanipulator 5171 (Eppendorf) connected to a microscope (model Axiovert-10; Carl Zeiss MicroImaging, Inc.). Cells were microinjected with 20 ng/μl DNA at 37°C. After 4 h at 37°C, the cells were surface stained with mAb 8D9 at 4°C for 15 min. The cells were washed with PBS^{2+}, fixed in 3% PFA in PBS^{2+}, and blocked in $Blocking\ Buffer_1$ (BB_1; 2% BSA [wt/vol] and 0.1% saponin [wt/vol] in PBS^{2+}) for 1 h. The cells were then stained with secondary antibodies in BB_1, washed in BB_1 for 30 min, and mounted on slides with DABCO anti-quench (50% glycerol [wt/vol] and 10% DABCO [wt/vol] in PBS^{2+}).

For in vivo inhibition of tyrosine kinase activity, MDCK cells were plated on 12-mm Transwell filters (0.4-μm pore size) at 4×10^5 cells/well 4 d before infection. The cells were then either mock infected or infected with AdNgCAM, AdCT3, or AdCT43 at 14 pfu/cell in 100 μl MEM for 1 h at 37°C. After 16 h infection, the cells were washed in PBS^{2+} and put into medium containing 12.5 μg/ml herbimycin A (Calbiochem). After 5 h at 37°C, the cells were surface stained at 4°C for 15 min with mAb 8D9 (NgCAM) or 6.23.3 (gp58). The cells were processed for immunofluorescence as described in the previous paragraph.

For LLC-PK1 expression experiments, the stably transfected cells were plated on 12-mm Transwell filters (0.4-μm pore size) at 4×10^5 cells/well. After 4 d, LLC-PK1::μ1A cells were infected at 7 pfu/cell, and LLC-PK1::μ1B cells at 14 pfu/cell. After 16 h, the cells were stained with mAb 8D9 or mAb C7 at 4°C for 15 min and processed for immunofluorescence.

For antibody uptake experiments, MDCK cells were plated on 12-mm Transwell filters (0.4-μm pore size) at 4×10^5 cells/well, 4 d before infection with either AdNgCAM or AdCT43. After 16 h, the basolateral chamber was washed with PBS^{2+} and refed with mAb 8D9-conditioned hybridoma supernatant, and the cells were incubated at 37°C for 30 min. The cells were then either fixed or growth medium added and incubated at 37°C for 2 h and then fixed. The cells were incubated in $Blocking\ Buffer_2$ (BB_2; 2% BSA [wt/vol] in PBS^{2+}) for 1 h, and stained for 1 h with secondary antibodies in BB_2. The cells were then washed in BB_2 for 30 min and processed for immunofluorescence.

Cells were analyzed using a confocal microscope (Microsystem LSM; Carl Zeiss MicroImaging, Inc.) with an Axiovert 100 microscope and a Plan-Neofluar 40× oil immersion objective (Carl Zeiss MicroImaging, Inc.). Images were acquired with LSM software. Images were then processed to adjust brightness and contrast using Adobe Photoshop.

In vitro phosphorylation of GST fusion proteins

4 μg GST fusion protein in 4 μl PBS^{2+} was mixed on ice with 4 μl of 4× SrcRB (125 mM $MgCl_2$, 25 mM $MnCl_2$, 2 mM EGTA, 0.25 mM sodium orthovanadate, 2 mM DTT, and 100 mM Tris-HCl, pH 7.2; Upstate Biotechnology), 7.3 U of his-p60src (Upstate Biotechnology), and 4 μl of 20 mM ATP and PBS^{2+} to a total volume of 20 μl. The samples were incubated at 30°C for 30 min and then analyzed by SDS-PAGE and Western blotting using a polyclonal antiphosphotyrosine antibody (Upstate Biotechnology). Blots were developed using ECL Plus Western Blotting Detection Reagents (GE Healthcare).

shRNA/RNA interference

Canine cDNAs for μ1A and μ1B were cloned from an MDCK cDNA library that was constructed according to manufacturer's specifications (Invitrogen). Oligonucleotides encoding an shRNA specifically directed against μ1B were designed, annealed, and cloned into pSUPER at the BglII–HindIII sites (Brummelkamp et al., 2002). The sequence of the oligonucleotides was as follows: 5′-GATCCCCGCAGTCAGTGGCCAATGGTTTCAAGAGAACCATTGGCCACTGACTGCTTTTTGGAAA-3′ and 5′-AGCTTTTCCAAAAAGCAGTCAGTGGCCAATGGTTCTCTTGAAACCATTGGCCACTGACTGCGGG-3′. An EcoRI–XhoI fragment, containing the H1 promoter and shRNA, was then transferred into RVH1-puromycin (Barton and Medzhitov, 2002; Schuck et al., 2004). Production of the recombinant virus and infection of MDCK cells was performed by a modification of the method of Schuck et al. (2004). 24 h after infection, stable clones were selected with MEM (Invitrogen) supplemented with 10% FBS, 2 mM L-glutamine, 100 U/ml penicillin, 100 μg/ml streptomycin, and 4 μg/ml puromycin (Sigma-Aldrich).

For Western blot analysis, cells grown in a 10-cm dish were scraped in 900 μl of lysis buffer (150 mM NaCl, 1% Triton X-100, 0.5% deoxycholate, 1× cOmplete Protease Inhibitor Cocktail with EDTA [Roche], and 50 mM Tris, pH 7.5) and passaged 4× through a 22-guage needle. The samples were transferred to microcentrifuge tubes and incubated for 30 min on ice. The samples were then spun at 16,000 *g* for 15 min at 4°C, and the supernatants were transferred to new tubes and supplemented with 0.1% SDS. A BCA protein assay (Pierce Chemical Co.) was performed and 72 μg of total protein from each sample was loaded onto an 8% polyacrylamide gel and analyzed by SDS-PAGE and Western blotting. Rabbit polyclonal antibodies against μ1A and μ1B were generated against peptides CVKAKSQFKRRSTANNV and CEKEEVEGRPPIGV, respectively, and affinity purified. An antibody against annexin II was obtained from BD Biosciences.

For immunofluorescence, 4×10^5 cells were plated onto 12-mm clear Transwell filters (0.4-μm pore size; Corning, Inc. Life Sciences) and allowed to grow for 4 d with daily changes of media. Cells were then infected with AdCT43. 20 h after infection, surface protein was labeled with anti-NgCAM 8D9 antibody for 15 min on ice. Samples were fixed and processed for immunofluorescence (as previously described in the Immunofluorescence section) using a goat anti–mouse Alexa 594 secondary antibody (Molecular Probes) and analyzed using a 510 confocal microscope (Carl Zeiss MicroImaging, Inc.).

We are grateful to B. Foellmer and S. Cox for technical assistance throughout all stages of this work. We are also grateful to D. Wisco, C. Norden, and G. Warren for advice on experimental design. We thank P. Sonderegger for providing critical reagents. We thank M. Velleca for making the MDCK cDNA library and T. Taguchi and S. Francis for making the μ1A and μ1B antibodies. We also thank G. Thomas, S. Arch, and members of the Mellman-Warren laboratory for helpful discussions.

This work was supported by a National Institutes of Health grant (GM29765) and by the Ludwig Institute for Cancer Research (I. Mellman). E. Anderson was supported by a Research Scholar Grant (PF-01-092-01-CSM) from the American Cancer Society. B. Winckler was supported by a Basil O'Connor Scholarship (March of Dimes Foundation) and a Scientist Development grant from the American Heart Foundation.

Submitted: 8 June 2005
Accepted: 7 July 2005

References

Ang, A.L., T. Taguchi, S. Francis, H. Fölsch, L.J. Murrells, M. Pypaert, G. Warren, and I. Mellman. 2004. Recycling endosomes can serve as intermediates during transport from the Golgi to the plasma membrane of MDCK cells. *J. Cell Biol.* 167:531–543.

Apodaca, G., L.A. Katz, and K.E. Mostov. 1994. Receptor-mediated transcytosis of IgA in MDCK cells is via apical recycling endosomes. *J. Cell Biol.* 125:67–86.

Aroeti, B., and K. E. Mostov. 1994. Polarized sorting of the polymeric immunoglobulin receptor in the exocytotic and endocytotic pathways is controlled by the same amino acids. *EMBO J.* 13:2297–2304.

Aroeti, B., P.A. Kosen, I.D. Kuntz, F.E. Cohen, and K.E. Mostov. 1993. Mutational and secondary structural analysis of the basolateral sorting signal of the polymeric immunoglobulin receptor. *J. Cell Biol.* 123:1149–1160.

Barroso, M., and E.S. Sztul. 1994. Basolateral to apical transcytosis in polarized cells is indirect and involves BFA and trimeric G protein sensitive passage through the apical endosome. *J. Cell Biol.* 124:83–100.

Barton, G.M., and R. Medzhitov. 2002. Retroviral delivery of small interfering RNA into primary cells. *Proc. Natl. Acad. Sci. USA.* 99:14943–14945.

Bonifacino, J.S., and L.M. Traub. 2003. Signals for sorting of transmembrane proteins to endosomes and lysosomes. *Annu. Rev. Biochem.* 72:395–447.

Brummelkamp, T.R., R. Bernards, and R. Agami. 2002. A system for stable expression of short interfering RNAs in mammalian cells. *Science.* 296: 550–553.

Burgoon, M.P., M. Grumet, V. Mauro, G.M. Edelman, and B.A. Cunningham. 1991. Structure of the chicken neuron-glia cell adhesion molecule, Ng-CAM: origin of the polypeptides and relation to the Ig superfamily. *J. Cell Biol.* 112:1017–1029.

Casanova, J.E., P.P. Breitfeld, S.A. Ross, and K.E. Mostov. 1990. Phosphorylation of the polymeric immunoglobulin receptor required for its efficient transcytosis. *Science.* 248:742–745.

Casanova, J.E., G. Apodaca, and K.E. Mostov. 1991. An autonomous signal for basolateral sorting in the cytoplasmic domain of the polymeric immunoglobulin receptor. *Cell.* 66:65–75.

Cheng, L., K. Itoh, and V. Lemmon. 2005. L1-mediated branching is regulated by two ezrin-radixin-moesin (ERM)-binding sites, the RSLE region and a novel juxtamembrane ERM-binding region. *J. Neurosci.* 25:395–403.

Dahlin-Huppe, K., E.O. Berglund, B. Ranscht, and W.B. Stallcup. 1997. Mutational analysis of the L1 neuronal cell adhesion molecule identifies membrane-proximal amino acids of the cytoplasmic domain that are required for cytoskeletal anchorage. *Mol. Cell. Neurosci.* 9:144–156.

Davis, J.Q., T. McLaughlin, and V. Bennett. 1993. Ankyrin-binding proteins related to nervous system cell adhesion molecules: candidates to provide transmembrane and intercellular connections in adult brain. *J. Cell Biol.* 121:121–133.

Dickson, T.C., C.D. Mintz, D.L. Benson, and S.R. Salton. 2002. Functional binding interaction identified between the axonal CAM L1 and members of the ERM family. *J. Cell Biol.* 157:1105–1112.

Doherty, P., G. Williams, and E.J. Williams. 2000. CAMs and axonal growth: a critical evaluation of the role of calcium and the MAPK cascade. *Mol. Cell. Neurosci.* 16:283–295.

Drubin, D.G., and W.J. Nelson. 1996. Origins of cell polarity. *Cell.* 84:335–344.

Elbashir, S.M., J. Harborth, W. Lendeckel, A. Yalcin, K. Weber, and T. Tuschl. 2001. Duplexes of 21-nucleotide RNAs mediate RNA interference in cultured mammalian cells. *Nature.* 411:494–498.

Esch, T., V. Lemmon, and G. Banker. 1999. Local presentation of substrate molecules directs axon specification by cultured hippocampal neurons. *J. Neurosci.* 19:6417–6426.

Felding-Habermann, B., S. Silletti, F. Mei, C.H. Siu, P.M. Yip, P.C. Brooks, D.A. Cheresh, T.E. O'Toole, M.H. Ginsberg, and A.M. Montgomery. 1997. A single immunoglobulin-like domain of the human neural cell adhesion molecule L1 supports adhesion by multiple vascular and platelet integrins. *J. Cell Biol.* 139:1567–1581.

Fölsch, H. 2005. The building blocks for basolateral vesicles in polarized epithelial cells. *Trends Cell Biol.* 15:222–228.

Fölsch, H., H. Ohno, J.S. Bonifacino, and I. Mellman. 1999. A novel clathrin adaptor complex mediates basolateral targeting in polarized epithelial cells. *Cell.* 99:189–198.

Fölsch, H., M. Pypaert, P. Schu, and I. Mellman. 2001. Distribution and function of AP-1 clathrin adaptor complexes in polarized epithelial cells. *J. Cell Biol.* 152:595–606.

Gut, A., F. Kappeler, N. Hyka, M.S. Balda, H.P. Hauri, and K. Matter. 1998. Carbohydrate-mediated Golgi to cell surface transport and apical targeting of membrane proteins. *EMBO J.* 17:1919–1929.

Hirt, R.P., G.J. Hughes, S. Frutiger, P. Michetti, C. Perregaux, O. Poulain-Godefroy, N. Jeanguenat, M.R. Neutra, and J.P. Kraehenbuhl. 1993. Transcytosis of the polymeric Ig receptor requires phosphorylation of serine 664 in the absence but not the presence of dimeric IgA. *Cell.* 74: 245–255.

Hortsch, M. 2000. Structural and functional evolution of the L1 family: are four adhesion molecules better than one? *Mol. Cell. Neurosci.* 15:1–10.

Hunziker, W., C. Harter, K. Matter, and I. Mellman. 1991. Basolateral sorting in MDCK cells requires a distinct cytoplasmic domain determinant. *Cell.* 66:907–920.

Ikonen, E., and K. Simons. 1998. Protein and lipid sorting from the trans-Golgi network to the plasma membrane in polarized cells. *Semin. Cell Dev. Biol.* 9:503–509.

Jareb, M., and G. Banker. 1998. The polarized sorting of membrane proteins expressed in cultured hippocampal neurons using viral vectors. *Neuron.* 20: 855–867.

Jenkins, S.M., K. Kizhatil, N.R. Kramarcy, A. Sen, R. Sealock, and V. Bennett. 2001. FIGQY phosphorylation defines discrete populations of L1 cell adhesion molecules at sites of cell-cell contact and in migrating neurons. *J. Cell Sci.* 114:3823–3835.

Kamiguchi, H., and V. Lemmon. 2000. IgCAMs: bidirectional signals underlying neurite growth. *Curr. Opin. Cell Biol.* 12:598–605.

Kamiguchi, H., K.E. Long, M. Pendergast, A.W. Schaefer, I. Rapoport, T. Kirchhausen, and V. Lemmon. 1998. The neural cell adhesion molecule L1 interacts with the AP-2 adaptor and is endocytosed via the clathrin-mediated pathway. *J. Neurosci.* 18:5311–5321.

Kizhatil, K., Y.X. Wu, A. Sen, and V. Bennett. 2002. A new activity of doublecortin in recognition of the phospho-FIGQY tyrosine in the cytoplasmic domain of neurofascin. *J. Neurosci.* 22:7948–7958.

Kleene, R., H. Yang, M. Kutsche, and M. Schachner. 2001. The neural recognition molecule L1 is a sialic acid-binding lectin for CD24, which induces promotion and inhibition of neurite outgrowth. *J. Biol. Chem.* 276: 21656–21663.

Koivisto, U.M., A.L. Hubbard, and I. Mellman. 2001. A novel cellular phenotype for familial hypercholesterolemia due to a defect in polarized targeting of LDL receptor. *Cell.* 105:575–585.

Luton, F., M.H. Cardone, M. Zhang, and K.E. Mostov. 1998. Role of tyrosine phosphorylation in ligand-induced regulation of transcytosis of the polymeric Ig receptor. *Mol. Biol. Cell.* 9:1787–1802.

Luton, F., M. Verges, J.P. Vaerman, M. Sudol, and K.E. Mostov. 1999. The SRC family protein tyrosine kinase p62yes controls polymeric IgA transcytosis in vivo. *Mol. Cell.* 4:627–632.

Matter, K. 2000. Epithelial polarity: sorting out the sorters. *Curr. Biol.* 10:R39–R42.

Matter, K., and I. Mellman. 1994. Mechanisms of cell polarity: sorting and transport in epithelial cells. *Curr. Opin. Cell Biol.* 6:545–554.

Matter, K., W. Hunziker, and I. Mellman. 1992. Basolateral sorting of LDL receptor in MDCK cells: the cytoplasmic domain contains two tyrosine-dependent targeting determinants. *Cell.* 71:741–753.

Matter, K., J.A. Whitney, E.M. Yamamoto, and I. Mellman. 1993. Common signals control low density lipoprotein receptor sorting in endosomes and the Golgi complex of MDCK cells. *Cell*. 74:1053–1064.

Mellman, I. 1996. Endocytosis and molecular sorting. *Annu. Rev. Cell Dev. Biol.* 12:575–625.

Mostov, K.E., and D.L. Deitcher. 1986. Polymeric immunoglobulin receptor expressed in MDCK cells transcytoses IgA. *Cell.* 46:613–621.

Mostov, K.E., M. Verges, and Y. Altschuler. 2000. Membrane traffic in polarized epithelial cells. *Curr. Opin. Cell Biol.* 12:483–490.

Nelson, W.J., and C. Yeaman. 2001. Protein trafficking in the exocytic pathway of polarized epithelial cells. *Trends Cell Biol.* 11:483–486.

Nolte, C., M. Moos, and M. Schachner. 1999. Immunolocalization of the neural cell adhesion molecule L1 in epithelia of rodents. *Cell Tissue Res.* 298: 261–273.

Ohno, H., T. Tomemori, F. Nakatsu, Y. Okazaki, R.C. Aguilar, H. Foelsch, I. Mellman, T. Saito, T. Shirasawa, and J.S. Bonifacino. 1999. Mu1B, a novel adaptor medium chain expressed in polarized epithelial cells. *FEBS Lett.* 449:215–220.

Okamoto, C.T., W. Song, M. Bomsel, and K.E. Mostov. 1994. Rapid internalization of the polymeric immunoglobulin receptor requires phosphorylated serine 726. *J. Biol. Chem.* 269:15676–15682.

Peles, E., J. Schlessinger, and M. Grumet. 1998. Multi-ligand interactions with receptor-like protein tyrosine phosphatase beta: implications for intercellular signaling. *Trends Biochem. Sci.* 23:121–124.

Polishchuk, R., A.D. Pentima, and J. Lippincott-Schwartz. 2004. Delivery of raft-associated, GPI-anchored proteins to the apical surface of polarized MDCK cells by a transcytotic pathway. *Nat. Cell Biol.* 6:297–307.

Reich, V., K. Mostov, and B. Aroeti. 1996. The basolateral sorting signal of the polymeric immunoglobulin receptor contains two functional domains. *J. Cell Sci.* 109:2133–2139.

Rodriguez-Boulan, E., and A. Gonzalez. 1999. Glycans in post-Golgi apical targeting: sorting signals or structural props? *Trends Cell Biol.* 9:291–294.

Roush, D.L., C.J. Gottardi, H.Y. Naim, M.G. Roth, and M.J. Caplan. 1998. Tyrosine-based membrane protein sorting signals are differentially interpreted by polarized Madin-Darby canine kidney and LLC-PK1 epithelial cells. *J. Biol. Chem.* 273:26862–26869.

Sampo, B., S. Kaech, S. Kunz, and G. Banker. 2003. Two distinct mechanisms target membrane proteins to the axonal surface. *Neuron.* 37:611–624.

Schaefer, A.W., H. Kamiguchi, E.V. Wong, C.M. Beach, G. Landreth, and V. Lemmon. 1999. Activation of the MAPK signal cascade by the neural cell adhesion molecule L1 requires L1 internalization. *J. Biol. Chem.* 274:37965–37973.

Schaefer, A.W., Y. Kamei, H. Kamiguchi, E.V. Wong, I. Rapoport, T. Kirch-

hausen, C.M. Beach, G. Landreth, S.K. Lemmon, and V. Lemmon. 2002. L1 endocytosis is controlled by a phosphorylation-dephosphorylation cycle stimulated by outside-in signaling by L1. *J. Cell Biol.* 157:1223–1232.

Scheiffele, P., J. Peranen, and K. Simons. 1995. N-glycans as apical sorting signals in epithelial cells. *Nature.* 378:96–98.

Schuck, S., A. Manninen, M. Honsho, J. Fullekrug, and K. Simons. 2004. Generation of single and double knockdowns in polarized epithelial cells by retrovirus-mediated RNA interference. *Proc. Natl. Acad. Sci. USA.* 101: 4912–4917.

Silletti, S., F. Mei, D. Sheppard, and A.M. Montgomery. 2000. Plasmin-sensitive dibasic sequences in the third fibronectin-like domain of L1–cell adhesion molecule (CAM) facilitate homomultimerization and concomitant integrin recruitment. *J. Cell Biol.* 149:1485–1502.

Simmen, T., M. Nobile, J.S. Bonifacino, and W. Hunziker. 1999. Basolateral sorting of furin in MDCK cells requires a phenylalanine- isoleucine motif together with an acidic amino acid cluster. *Mol. Cell. Biol.* 19:3136–3144.

Singer, K.L., and K.E. Mostov. 1998. Dimerization of the polymeric immunoglobulin receptor controls its transcytotic trafficking. *Mol. Biol. Cell.* 9:901–915.

Song, W., M. Bomsel, J. Casanova, J.P. Vaerman, and K. Mostov. 1994. Stimulation of transcytosis of the polymeric immunoglobulin receptor by dimeric IgA. *Proc. Natl. Acad. Sci. USA.* 91:163–166.

Stein, M., A. Wandinger-Ness, and T. Roitbak. 2002. Altered trafficking and epithelial cell polarity in disease. *Trends Cell Biol.* 12:374–381.

Tuma, P.L., and A.L. Hubbard. 2003. Transcytosis: crossing cellular barriers. *Physiol. Rev.* 83:871–932.

Tuvia, S., T.D. Garver, and V. Bennett. 1997. The phosphorylation state of the FIGQY tyrosine of neurofascin determines ankyrin-binding activity and patterns of cell segregation. *Proc. Natl. Acad. Sci. USA.* 94:12957–12962.

Verges, M., F. Luton, C. Gruber, F. Tiemann, L.G. Reinders, L. Huang, A.L. Burlingame, C.R. Haft, and K.E. Mostov. 2004. The mammalian retromer regulates transcytosis of the polymeric immunoglobulin receptor. *Nat. Cell Biol.* 6:763–769.

Vogt, L., R.J. Giger, U. Ziegler, B. Kunz, A. Buchstaller, W. Hermens, M.G. Kaplitt, M.R. Rosenfeld, D.W. Pfaff, J. Verhaagen, and P. Sonderegger. 1996. Continuous renewal of the axonal pathway sensor apparatus by insertion of new sensor molecules into the growth cone membrane. *Curr. Biol.* 6:1153–1158.

Walsh, F.S., and P. Doherty. 1997. Neural cell adhesion molecules of the immunoglobulin superfamily: role in axon growth and guidance. *Annu. Rev. Cell Dev. Biol.* 13:425–456.

Whitesell, L., E.G. Mimnaugh, B. De Costa, C.E. Myers, and L.M. Neckers. 1994. Inhibition of heat shock protein HSP90-pp60v-src heteroprotein complex formation by benzoquinone ansamycins: essential role for stress proteins in oncogenic transformation. *Proc. Natl. Acad. Sci. USA.* 91:8324–8328.

Winckler, B., and I. Mellman. 1999. Neuronal polarity: controlling the sorting and diffusion of membrane components. *Neuron.* 23:637–640.

Winckler, B., P. Forscher, and I. Mellman. 1999. A diffusion barrier maintains distribution of membrane proteins in polarized neurons. *Nature.* 397: 698–701.

Wisco, D., E.D. Anderson, M.C. Chang, C. Norden, T. Boiko, H. Fölsch, and B. Winckler. 2003. Uncovering multiple axonal targeting pathways in hippocampal neurons. *J. Cell Biol.* 162:1317–1328.

Wong, E.V., A.W. Schaefer, G. Landreth, and V. Lemmon. 1996. Involvement of p90rsk in neurite outgrowth mediated by the cell adhesion molecule L1. *J. Biol. Chem.* 271:18217–18223.